JOURNAL OF AGRICULTURAL AND FOOD CHEMISTRY

ARTICLE

pubs.acs.org/JAFC

Photoinduced Oxidation of the Insecticide Phenothrin on Soil Surfaces

Yusuke Suzuki,*[,†] Andrea Lopez,[§] Marian Ponte,[§] Takuo Fujisawa,[†] Luis O. Ruzo,[§] and Toshiyuki Katagi[†]

[†]Environmental Health Science Laboratory, Sumitomo Chemical Company, Ltd., 4-2-1 Takatsukasa, Takarazuka, Hyogo 665-8555, Japan

[§]PTRL-West, Inc., 625-B Alfred Novel Drive, Hercules, California 94547, United States

ABSTRACT: Photodegradation profiles of the pyrethroid insecticide phenothrin on a moistened U.S. soil thin layer was investigated by using its predominant component, the 1*R*-*trans*-isomer (**I**), under continuous exposure to light at >290 nm from a xenon arc lamp. Its degradation was moderately accelerated by irradiation with half-lives of 5.7−5.9 days (dark control 21−24 days), mainly via successive oxidation of the 2-methylprop-1-enyl group and ester cleavage followed by mineralization to carbon dioxide. Spectroscopic and cochromatographic analyses showed that the major degradates were the alcohol and ketone derivatives of **I** formed via photoinduced oxidation of the 2-methylprop-1-enyl group by singlet oxygen. The photoinduced generation of singlet oxygen in/on the soil surface was confirmed by using chemical trapping reactions together with ESR spectroscopy.

KEYWORDS: pyrethroid, phenothrin, photo-oxidation, singlet oxygen, ESR

INTRODUCTION

Photochemical transformation of pesticides on soil surfaces is one of the most important dissipation routes either after the direct application of pesticides or through spray drift and wash-off from plants by rain. The direct photolysis rate of pesticides in/on soil surfaces is substantially slower than that in the aqueous phase mainly due to light attenuation by soil,[1] whereas indirect mechanisms such as photoinduced oxidation by reactive oxygen species are known to play an important role in the degradation of many pesticides.[2] The photosensitized generation of highly reactive singlet oxygen ($^1O_2$) has been reported not only in natural waters[3,4] but also on soil surfaces.[5,6] The electrophilicity of $^1O_2$ leads to reactions at the electron-rich moieties of some pyrethroids such as the 2-methylprop-1-enyl group in chrysanthemic acid[7] and the furfuryl alcohol groups.[8,9] Other reactive species such as atmospheric ozone also enhance their degradation via ozonolysis or epoxidation to finally yield the corresponding aldehyde and carboxylic acid.[10,11]

Phenothrin [3-phenoxybenzyl (1*RS*)-*cis*−*trans*-2,2-dimethyl-3-(2-methylprop-1-enyl)cyclopropanecarboxylate] is an early-generation synthetic pyrethroid developed by Sumitomo Chemical Co., Ltd.[12] The 1*R*-*trans* isomer of phenothrin exhibits the highest insecticidal activity among its four possible isomers derived from two chiral carbons at the 1- and 3-positions of the cyclopropane ring. Sumithrin (*d*-phenothrin), *cis*/*trans* = 20:80 and 1*R*-isomer >95%, has been widely used as an insect knockdown agent for indoor and outdoor usages.[13] Although the use pattern of phenothrin is limited to noncrop areas, the possibility of its release to the environment should be envisaged in case of residential exposures from outdoor lawn and garden sprays against groundling or flying insect pests. Several studies on phenothrin have been carried out to assess its environmental fate[14,15] as well as mammalian and fish metabolism.[16,17] Furthermore, the identities of its transformation products in air and on surface samples taken following indoor applications have been reported by using high-resolution gas chromatography and mass spectrometry.[18,19] However, much less information is currently available for its photodegradation behavior including oxidation mechanisms on soil surfaces because of its very limited entry into the environment.

The aim of this study was to determine the photodegradation profiles of phenothrin in/on a typical California sandy clay loam soil. The 1*R*-*trans* isomer (**I**), as a major constituent of *d*-phenothrin, labeled with ^{14}C in either the acid or alcohol moiety, was applied to the test soil and continuously irradiated by artificial sunlight from a xenon arc lamp. The photoinduced oxidation by $^1O_2$ is thought to be one of the potential degradation mechanisms of **I** on soil surface. Therefore, the generation of $^1O_2$ on the tested soil was first examined by trapping this species with 2,5-dimethylfuran.[20,21] Second, the photoinduced formation of $^1O_2$ in the presence of humic substances (HSs) extracted from the test soil was monitored by measuring the electron spin resonance (ESR) signal of the nitroxide radical originating from the reaction of $^1O_2$ with a specific spin label, 2,2,6,6-tetramethyl-4-piperidone.[22,23]

MATERIALS AND METHODS

Chemicals. The two radiolabels of **I**, individually labeled with ^{14}C at the 1-position of the cyclopropyl ring (CP-^{14}C, 5.8 MBq mg^{-1}) or uniformly at the phenoxyphenyl ring (PP-^{14}C, 12.5 MBq mg^{-1}), were synthesized in our laboratory.[12] The radiochemical and optical purities were determined to be >99.2% for both ^{14}C labels. The nonradiolabeled **I**, its isomers, and (1*R*)-*trans*-chrysanthemic acid (**II**) were prepared in our laboratory.[12,24] (1*R*)-*trans*-2,2-Dimethyl-3-(2-hydroxy-2-methyl-1-oxopropyl)cyclopropanecarboxylic acid (**III**) was synthesized from **II** using $KMnO_4$.[25] Three oxidized esters [**VII**, 3-phenoxybenzyl (1*R*)-*trans*-2,2-dimethyl-3-formylcyclopropanecarboxylate; **VIII**, 3-phenoxybenzyl (1*R*)-*trans*-2,2-dimethyl-3-carboxycyclopropanecarboxylate, and **IX**, 3-phenoxybenzyl (1*R*)-*trans*-2,2-dimethyl-3-[(1*RS*)-1-hydroxy-2-methylprop-2-enyl]cyclopropanecarboxylate] were prepared according

Received: June 28, 2011
Revised: August 26, 2011
Accepted: August 30, 2011
Published: August 30, 2011

to reported methods.[7,14] The keto derivative of **I** [**X**, 3-phenoxybenzyl (1*R*)-*trans*-2,2-dimethyl-3-(2-methyl-1-oxoprop-2-enyl)cyclopropanecarboxylate] was synthesized by treating **IX** with pyridinium chlorochromate in chloroform.[26] Crude **X** was purified by silica gel column chromatography using *n*-hexane/ethyl acetate (3:1, v/v) (purity = 93.0%). **X**: MS *m*/*z* 365 $(M + H)^+$; ^{1}H NMR (300 MHz, $CDCl_3$) δ 1.08−1.36 (s, 6H, CP-2-($C\underline{H}_3$)$_2$), 1.89 (s, 3H, $C\underline{H}_3CH(=CH_2)-$), 2.46−2.86 (s, 2H, CP-1,3-$\underline{H}$), 5.09 (s, 2H, Ar−$C\underline{H}_2O-$), 5.84−5.99 (s, 2H, $CH_3CH(=C\underline{H}_2)-$), 6.94−7.59 (m, 9H, Ar H). 3-Phenoxybenzyl alcohol (**III**), 3-phenoxybenzaldehyde (**IV**), 3-phenoxybenzoic acid (**V**), 2,5-dimethylfuran (DMF), 2,2,6,6-tetramethyl-4-piperidone, hydrochloride (TMPD), Rose Bengal (RB), and sodium azide (NaN_3) were purchased from Sigma-Aldrich (St. Louis, MO). All solvents and other reagents were obtained from Fisher Scientific International Inc. (Hampton, NH). All water used was HPLC grade or purified with a Barnstead NANOpure II system or Puric MX-II$_{AN}$ equipped with a G-10 filter (Organo Co., Tokyo, Japan).

Table 1. Chromatographic Properties of I and Its Related Degradates

	t_R[a] (min)		R_f[b]	
compound	1	2	A	B
1*R*-*trans*-phenothrin (**I**)	40.0	45.7	0.79	0.74
1*R*-*cis*-phenothrin	39.5	38.9	0.79	0.73
1*S*-*trans*-phenothrin	na[c]	47.5	na	na
1*S*-*cis*-phenothrin	na	41.5	na	na
II	18.8	na	0.55	0.43
III	9.7	na	0.00	0.00
IV	19.5	na	0.63	0.07
V	24.4	na	0.79	0.42
VI	20.5	na	0.32	0.08
VII	28.8	na	0.76	0.36
VIII	25.0	na	0.36	0.10
IX-a/IX-b	28.2/30.2	na	0.71/0.76	0.17
X	34.7	na	0.76	0.44

[a] Typical HPLC retention time: 1, reversed-phase HPLC; 2, chiral HPLC. [b] TLC R_f values with indicated solvent systems: A, chloroform/methanol (9:1, v/v); B, *n*-hexane/ethyl acetate/acetic acid (40:10:1, v/v/v). [c] Not analyzed.

Radioassay. The radioactivity in aliquots of organic extracts of soils, bound residues, and trapping media was individually determined by liquid scintillation counting (LSC) with a Beckman LS6500 or LS6000IC liquid scintillation spectrometer using 5 or 15 mL of liquid scintillation cocktail in a 7 or 20 mL standard polyethylene counting vial. The unextractable soil residues were combusted at least in triplicate using a Harvey biological sample oxidizer, followed by LSC. The amounts of ^{14}C collected in the NaOH traps were determined as $^{14}CO_2$ by adding $BaCl_2$, resulting in the quantitative precipitation as $Ba^{14}CO_3$. Typical parameters are as follows: counting efficiency, 98%; background, 1 Bq; counting time, 1 min.

Chromatography. Soil extracts were analyzed by reversed-phase high-performance liquid chromatography (HPLC) for both quantification and identification of **I** and its degradates. An Agilent 1100 or 1200 series HPLC Chemstation chromatography system equipped with a Capsell-Pack C18 UG 120 (4.6 mm i.d. × 150 mm) was operated at a flow rate of 1 mL min^{-1} using a mobile phase stepwise changing as

Table 2. Distribution of Radioactivity of I and Its Degradates on Soil Surfaces

	% of applied ^{14}C									
	[CP-^{14}C]-**I**					[PP-^{14}C]-**I**				
	light			dark		light			dark	
	1 day	5 days	13 days	5 days	13 days	1 day	6 days	12 days	6 days	12 days
neutral extract ^{14}C	95.8	81.7	65.3	97.1	84.5	95.3	82.6	67.5	92.4	79.2
I	69.5	40.1	19.8	90.7	71.4	62.0	29.5	21.7	79.9	61.8
isomers of **I**[a]	0.7	0.6	0.1	0.5	0.5	0.3	0.2	0.4	1.4	0.6
II	0.4	0.8	0.4	0.8	1.0	–[b]	–	–	–	–
III	nd[c]	0.3	0.2	nd	nd	–	–	–	–	–
IV	–	–	–	–	–	2.6	2.2	1.3	nd	0.2
V	–	–	–	–	–	0.8	0.6	0.7	nd	nd
VI	–	–	–	–	–	3.2	8.1	7.8	7.2	6.3
VII	2.6	0.9	0.5	nd	0.5	3.5	1.7	0.8	nd	nd
VIII	1.5	2.4	2.5	nd	nd	2.0	3.2	2.5	nd	nd
IX-a	2.8	5.7	4.0	0.5	1.2	3.1	5.7	4.2	2.3	1.9
IX-b	2.4	4.1	2.7	nd	0.2	2.3	4.2	3.0	nd	nd
X	7.5	8.9	5.4	nd	nd	7.7	9.0	6.4	nd	nd
others[e]	8.7	18.0	29.8	4.7	10.0	7.9	18.5	19.1	1.6	8.6
acidic/exhaustive extract ^{14}C	na	3.1	7.8	na[d]	2.1	na	4.3	10.6	na	5.6
bound residue	6.4	10.6	18.9	6.6	10.6	6.1	12.9	17.9	10.8	13.0
volatiles ($^{14}CO_2$)	0.8	4.6	11.1	3.0	2.0	0.1	2.6	4.3	1.1	4.0
total ^{14}C	103.0	100.0	103.0	106.7	99.1	101.5	102.4	100.2	104.2	101.7

[a] Three other isomers of **I** detected in C_{18} and Chiral HPLC analyses. [b] Not detectable due to the labeled position. [c] Not detected. [d] Not analyzed. [e] Consisted of multiple degradates, each of which amounted to less than 2.7%AR.

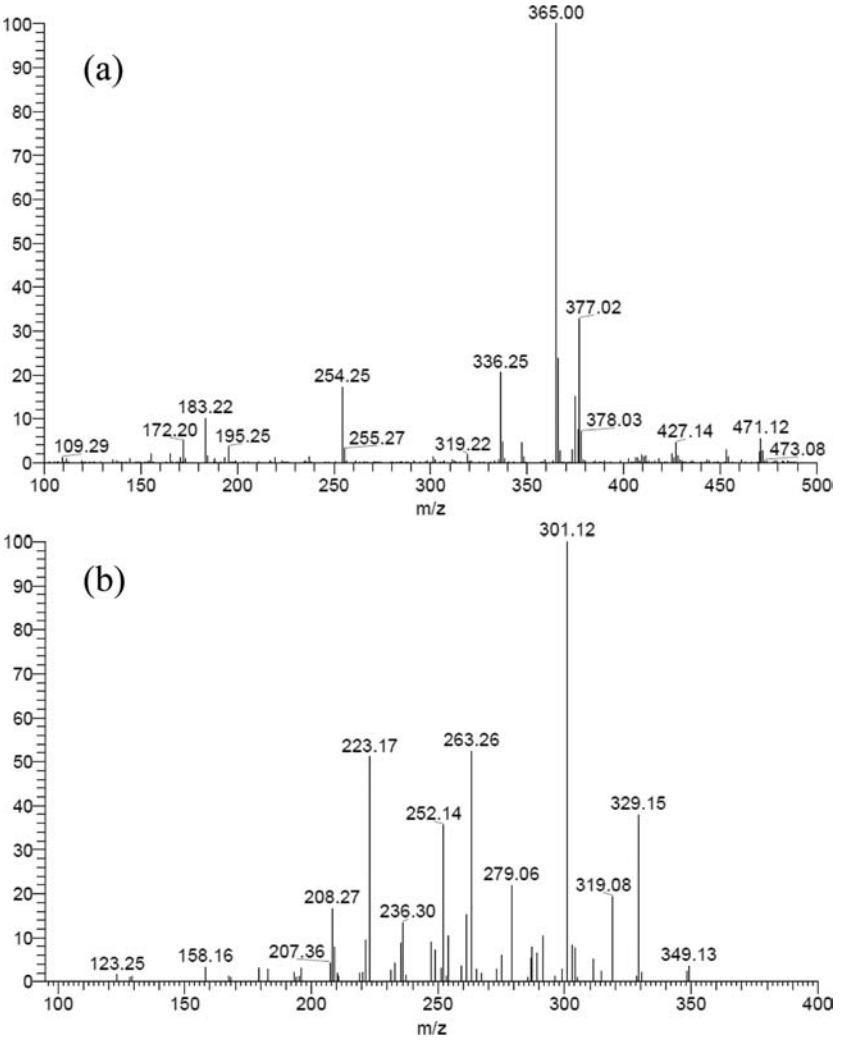

Figure 1. LC-MS (a) and MS/MS (b) spectra of **X** extracted from [PP-^{14}C]-**I** soil sample.

follows: 0 min, % A (0.1% trifluoroacetic acid in water)/% B (0.1% trifluoroacetic acid in acetonitrile), 90:10; 0−10 min, linear, 45:55 at 10 min; 10−40 min, linear, 5:95 at 40 min; 40−45 min, isocratic, 5:95 at 45 min; 45−46 min, linear, 90:10 at 46 min; 46−50 min, isocratic, 90:10 at 50 min. Chiral HPLC analysis was conducted by using two successive SUMICHIRAL OA-2000 (5 μm, 4-mm i.d. × 250 mm; Sumika Chemical Analysis Service, Ltd. (SCAS)., Osaka, Japan) columns operated with an isocratic mobile phase of *n*-hexane at a flow rate of 0.5 mL min^{-1}. The radioactivity of the column effluent was monitored with an IN/US Beta-ram ^{14}C flow-through detector. HPLC radiochromatograms were generated using LSC of the collected eluting fractions (0.3−0.5 min). Each ^{14}C peak was identified by HPLC cochromatography by comparing its retention time with those of nonradiolabeled reference standards being detected at 230 nm with an Agilent 1100 or 1200 series variable-wavelength detector. To further confirm the chemical identity of each degradate, two-dimensional thin-layer chromatography (2D-TLC) was conducted using silica gel 60F_{254} thin-layer plates (200 × 200 mm, 0.25 mm layer thickness; VWR, Com) with the solvent systems of A (chloroform/methanol; 9:1, v/v) and B (*n*-hexane/ethyl acetate/acetic acid; 40:10:1, v/v/v). The solvent system of toluene saturated with formic acid/diethyl ether (10:3, v/v) was used in 1D-TLC analysis for identification of **X** (R_f 0.68). Radioactive regions on the TLC plates were located and quantified with a Molecular Dynamics Storm 820 optical scanner (Sunnyvale, CA). Nonradiolabeled reference standards were visualized using shortwave UV. Typical retention times and R_f values of **I** and related degradates are listed in Table 1. DMF was analyzed and quantified by HPLC, using a standard curve in the range of 3.2−162 mg/L. A Hitachi L-2130 pump linked in series with an L-2400 UV detector at 230 nm was equipped with a Sumipax ODS A-212 column (150 × 6 mm i.d., 5 μm, SCAS) and operated at a flow rate of 1 mL min^{-1} in the following gradient mode: 0 min, % A (water)/%B (acetonitrile), 95:5; 0−20 min, linear, 5:95 at 20 min; 20−25 min, isocratic, 5:95 at 25 min.

Spectroscopy. Liquid chromatography−mass spectrometry (LC-MS) and LC-MS/MS with a collision energy of 35 V in positive and negative ion modes were performed by a Finnigan LCQ ion trap or a Waters ZQ 2000 mass spectrometer equipped with an atmospheric pressure chemical ionization (APCI) interface, being connected to an Agilent or Waters Alliance HPLC systems. Samples dissolved in an appropriate solvent were injected at a flow rate of 0.2 mL min^{-1} using the same gradient system as HPLC analyses. NMR spectra were measured in $CDCl_3$ with a Bruker AV 300 M NMR spectrometer operating at 300.13 MHz for proton NMR measurement using tetramethylsilane as an internal standard. ESR spectra were measured on a JEOL JES-100 ESR spectrometer (Tokyo, Japan) at room temperature using a Mn^{2+}/MgO marker as an internal standard. The analytical conditions were as follows: modulation frequency, 100 kHz; modulation amplitude, 70 μT, scanning field, 335.4 ± 5 mT; response time, 0.1 s;

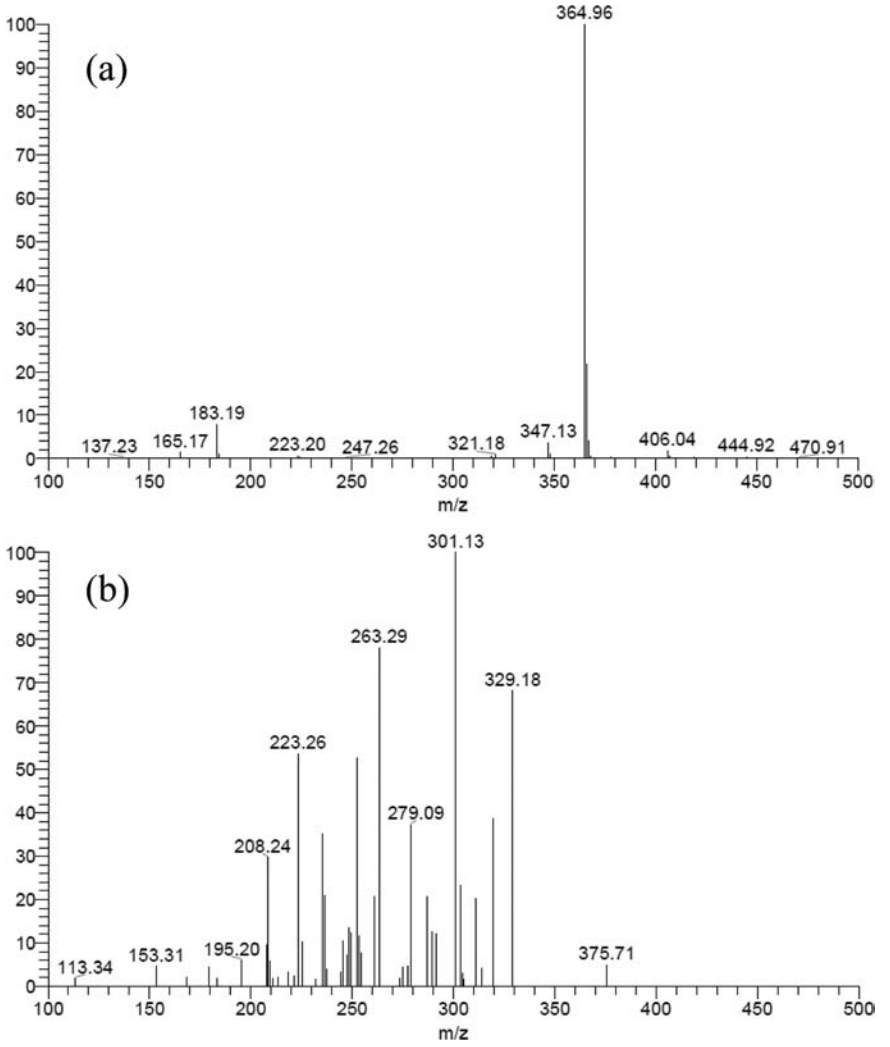

Figure 2. LC-MS (a) and MS/MS (b) spectra of synthetic reference standard **X**.

sweep time, 1.0 min; microwave power, 10 mW; microwave frequency, 9.4 GHz.

Soil Photolysis Study. A sandy clay loam soil collected from an experimental field in California [USDA classification; sand, 62%; silt, 17%; clay, 21%; organic matter, 1.8%; pH (H_2O), 6.5; moisture at one-third bar, 17.1%] was air-dried and passed through a 2 mm sieve prior to use to remove stones and plant debris. Soil samples of 3.1 g on a dry-weight basis were placed in quartz and Pyrex glass dishes with a 50-mm diameter for irradiated and dark samples, respectively. Deionized water was added to prepare an approximately 2 mm thickness of soil slurry, which was dried with a gentle stream of air to obtain an even thin layer of soil at a 75% field moisture capacity at one-third bar. Because the application rate of phenothrin in the field could not be simply defined due to its noncrop usage, the worst-case scenario was supposed as a single spray of 1.5 oz (42.5 g) as an outdoor residential fogging containing 0.15% (w/w) of phenothrin to a 1000 ft^2 field, resulting in an application rate of 7.3 g ai/ha. From the soil dish surface area of 19.6 cm^2 and 3.1 g dry weight soil per dish, 3 times the normal rate (1.5 μg/g) was applied to obtain sufficient amounts of degradates for identification. A 50 μL aliquot of acetonitrile solution of each [^{14}C]-**I** (94 mg L^{-1}) was added with a glass syringe directly to the soil surface in a spiral motion. The vessels containing treated soil thin-layer samples were connected to their respective volatile traps and irradiated continuously for 13 days using a Heraeus Suntest CPS+ unit equipped with a xenon lamp through a quartz glass filter with an IR-reflective coating and a special UV glass filter blocking the radiation below approximately 290 nm. The spectral distribution of the xenon lamp was similar to that of natural sunlight, and the averaged light intensities measured

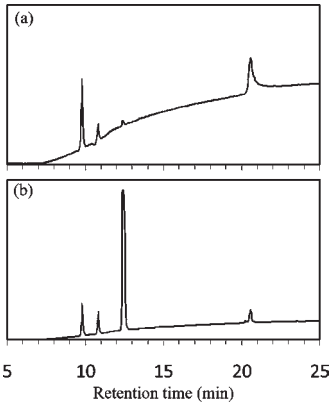

Figure 3. HPLC chromatograms of DMF and its photo-oxidation products: (a) on soil surface after 7 h; (b) in the aqueous solution containing RB after 1 h.

by a LI-COR LI-1800 spectroradiometer were 43.9 and 424 W/m^2 for the ranges of 300−400 and 300−800 nm, respectively. Light-exposed samples were placed in a water bath maintained at 20 ± 1 °C by a continuous circulation unit. A dark control experiment was separately conducted similarly as above except that the Pyrex reaction vessels were wrapped with aluminum foil to prevent light exposure and placed in an incubator maintained at 20 ± 1 °C. Sterile, moistened, and CO_2-free air was gently passed through the headspace of each soil sample and into a series of volatile traps including polyurethane foam plugs to collect organic volatiles and two 10% aqueous NaOH solutions for trapping CO_2. The soil moisture content was adjusted to its original level (if needed) by dropwise addition of deionized water every 1−3 days.

At each of five sampling times, soil thin-layer samples were taken in duplicate and subsequently extracted twice with 10 mL of methanol with a wrist action shaker for 10 min followed by centrifugation at 3000 rpm for 10 min. Mechanical extraction was additionally conducted with 10 mL of methanol/water (1:1, v/v) for 1 h. These extracts were combined (neutral extract), and the remaining soil, which contained >10% of the applied ^{14}C, was further extracted twice with methanol/0.2 M HCl (1:1, v/v) for 1 h. Exhaustive extractions were conducted for selected samples by refluxing with methanol/0.2 M HCl (1:1, v/v) for 3 h (acidic extracts). A 0.1−0.5 mL aliquot of each extract was taken for radioassay in triplicate by LSC, and then all neutral and acidic extracts at the final sampling were diluted with water (1:1) and subjected to HPLC cochromatographic analysis. Aliquots of selected soil extracts were also comigrated on 2D-TLC analysis with reference standards. In addition to the cochromatogaphic analyses, LC-MS spectra and MS/MS fragment patterns of the isolated **X** from soil extracts were compared with those of its reference standard. To obtain more robust evidence for the structure of the acid and alcohol moieties in **X**, isolated fractions from HPLC originating from both radiolabels were hydrolyzed with 0.1 M NaOH for up to 17 h at 25 °C under N_2. A portion of the hydrolysates was subjected to HPLC cochromatography with the corresponding reference standards (**II**, **III**, and **IV**) and to LC-MS analysis. To examine the possible isomerization of **I**, its isolated HPLC peak in selected neutral extracts was dissolved into *n*-hexane and subjected to chiral HPLC analysis. A portion of the soil containing unextracted radiocarbon was combusted using a sample oxidizer to determine the remaining bound ^{14}C residues on the soil. Selected postextraction soils at the final sampling for each label were further fractionated into humin, humic acid, and fulvic acid partitions according to the alkaline extraction−acid precipitation method.[27]

Assay of Singlet Oxygen ($^1O_2$). The generation of $^1O_2$ on the irradiated soil was examined according to a reported method.[5] A 200 μL aliquot of an acetonitrile solution of DMF (17.5 mg mL^{-1}) was evenly added to the tested soil thin layer (1 g), which was prepared on glass dishes (28 mm diameter) and the soil water content was adjusted as in the case of the soil photolysis experiment. The prepared soil dishes were sealed with a Pyrex glass cover and irradiated with a 2 kW xenon lamp (Ushio Inc., Tokyo, Japan) for 7 h. During irradiation, the temperature of the soil surface was maintained at 20 ± 3 °C by circulating thermostated water under the sample dishes. The irradiated soil samples were mechanically extracted twice with 10 mL of methanol for 5 min followed by centrifugation at 2500 rpm for 10 min. A 10 μL portion of supernatant diluted with methanol to 20 mL was subjected to HPLC analysis. A dark control sample concurrently prepared as above was wrapped in aluminum foil and placed in an incubator maintained at 20 °C. Reaction products of DMF with $^1O_2$ generated by a well-known photosensitizing dye, RB, were assessed to compare its photo-oxidation on the soil surface. A glass-capped 1 cm quartz cuvette containing a 50% acetonitrile aqueous solution of 4 mM DMF and 0.01 mM RB was irradiated with a 500 W xenon lamp (Ushio Inc.) through a Pyrex glass and heat absorption HA-50 filter (HOYA Optics, Tokyo, Japan) for 1 h under air at room temperature. Alternatively, the generation of $^1O_2$ from

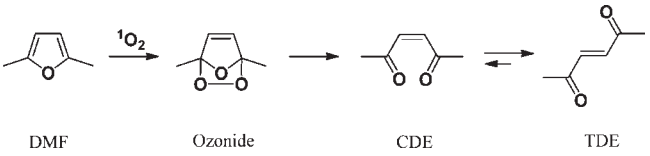

Figure 4. Reaction scheme of DMF with singlet oxygen ($^1O_2$).

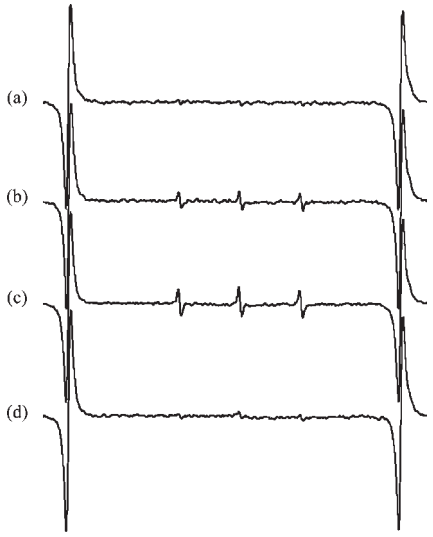

Figure 5. ESR spectra of TMPD (5 mM) aqueous solutions containing each soil-extracted HSs after 15 min of irradiation: (a) without HSs as control; (b) with OMs fraction; (c) with HA fraction; (d) with HA fraction and NaN_3.

the tested soil was examined by using HSs extracted from the test soil. According to the IHSS method,[27] the organic matters (OMs) fraction was obtained by extraction of 2 g of soil with 0.1 M NaOH (20 mL) for 4 h followed by acidification to separate humic acid (HA) precipitates. An appropriate amount of each fraction, whole OMs (1 mL) and HA (50 mg), was individually added to 10 mL of 0.05 M phosphate buffer (pH 7.89)/acetonitrile (4:1, v/v) in the presence of 5 mM TMPD. The final pH of each solution was adjusted to 7.98−8.02 by the addition of 0.1 M HCl or 0.1 M NaOH. The resulting solutions were aspirated into a flat quartz ESR cuvette (LLC-04B, LABOTEC., Tokyo, Japan), and ESR spectra were measured under irradiation with a 500 W xenon lamp through Pyrex and HA-50 filters for 15 min at room temperature.

RESULTS

Distribution of Radiocarbon and Degradation Rates of I. The distribution of radioactivity among neutral and acidic/exhaustive extracts, unextractable bound residues, and volatiles is summarized in Table 2. The total recovery of the applied radioactivity (AR) was 95.2−106.7% throughout the study. On irradiation, neutral extractable ^{14}C gradually decreased to 65.3−67.5% AR with concomitant increases in the acidic extracts and bound residues, amounting to 7.8−10.6 and 17.9−18.9% AR at the end of study, respectively. Selected samples containing unextracted ^{14}C for both labels were similarly fractionated into humin (7.9−8.2% AR), humic acid (4.7−5.0% AR), and fulvic acid (4.6−6.3% AR). The acid moiety of **I** was found to be gradually mineralized to $^{14}CO_2$, amounting to 11.1% AR at the end of exposure, whereas its alcohol moiety was less mineralized (4.3% AR). Trace amounts of volatiles except for $^{14}CO_2$ were

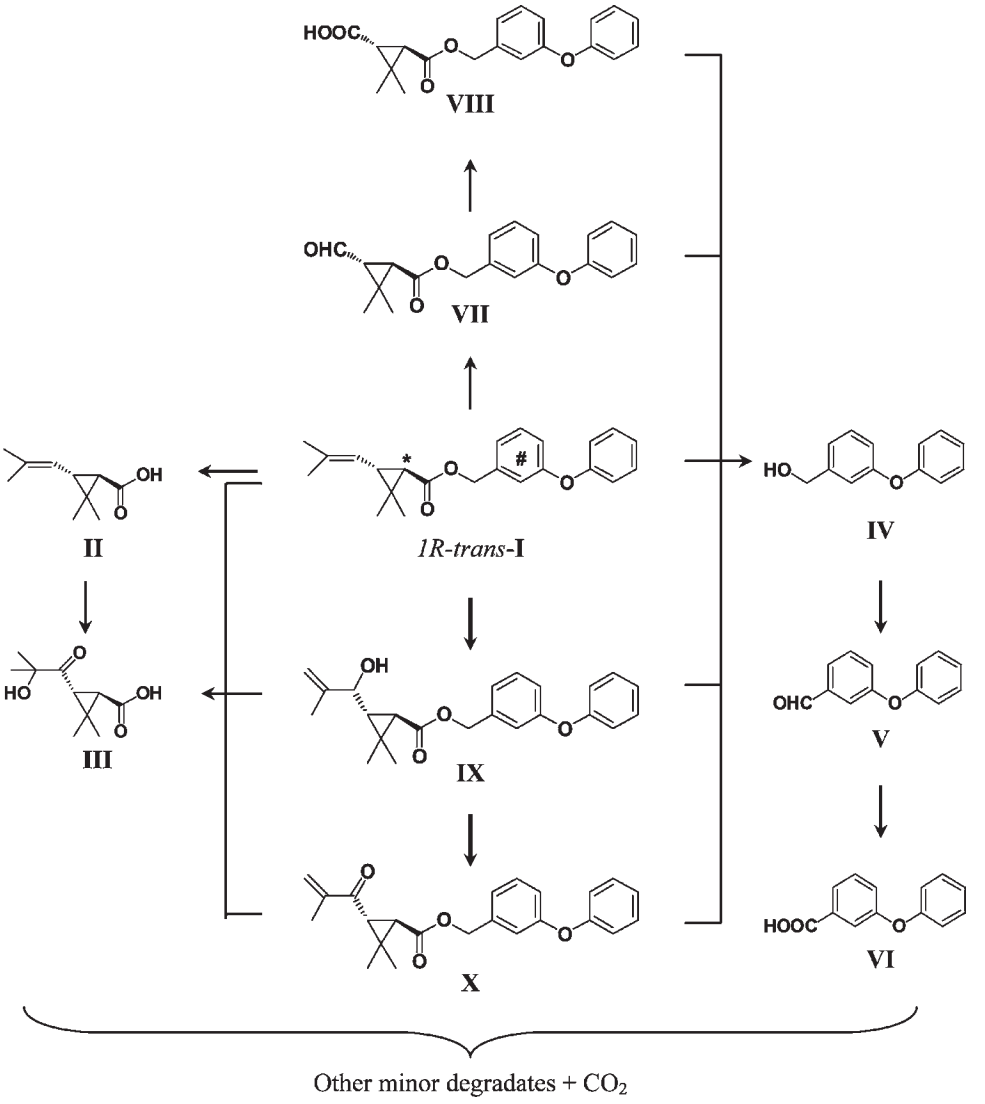

Figure 6. Photodegradation pathways of **I** on soil surface. ^{14}C labeled positions of **I**: ∗, [CP-^{14}C]-**I**; #, [PP-^{14}C]-**I**.

formed throughout the study (<0.1% AR). Under dark conditions, a decline of ^{14}C recovery upon extraction was observed, but >79.2% AR was still obtained in the neutral fractions throughout the study. Both the formation of bound residues and mineralization were less than those for the irradiated samples of each label, amounting to 10.6−13.0 and 4.0−6.5% AR, respectively. **I** degraded moderately on the soil surface with remaining amounts at 19.8−21.7% AR (irradiated) and 61.8−71.4% AR (dark control) over the experimental period. Single first-order kinetics applied to the disappearance of **I** determined by HPLC analysis of neutral soil extracts led to the calculation of half-lives under irradiated and dark conditions of 5.7−5.9 and 21−24 days, respectively.

Degradation Products of I on Soil Surface. One of the photoproducts common to both labels was **IX**, which exhibited two isomer peaks designated **IX-a** (28.2 min) and **IX-b** (30.2 min) originating from optical isomerism at the 1-position of the 2-methylprop-2-enyl-1-ol moiety, increased to 9.8−9.9% AR after 5−6 days of irradiation and finally declined to 6.7−7.2% AR. Slightly more **IX-a** than **IX-b** was formed by irradiation, and **IX-a** was also detected in trace amounts under dark conditions (<2.3% AR). Product **X** was also detected as a common photoproduct for both labels having a molecular weight of 364 amu as evidenced from its LC-MS signals at m/z 365 $[M + H]^+$ and 377 $[M(^{14}C) + H]^+$ for the PP-label (Figure 1a). Compound **X** was the only degradate at >10% AR after 3 days in the light-exposed samples, but declined to 5.4−6.4% AR at the end of irradiation. LC-MS and MS/MS fragment patterns of the corresponding authentic standard were in good agreement with those of the material isolated from soil extracts, as shown in Figures 1 and 2. Furthermore, HPLC cochromatographic analysis of hydrolysates of **X** showed a single peak (**IV**) for the PP-label, but neither **II** nor **III** was detected from the CP-label. The LC-MS spectrum of the main hydrolysate from the CP-label in positive APCI mode showed the parent peak at m/z 185 $[M(^{14}C) + H]^+$ with a daughter ion at m/z 164 $[M(^{14}C) - OH]^+$, indicating that the isolated peak from each label was conclusively identified as **X** formed through oxidation at the 2-methylprop-1-enyl group of the acid moiety. The other oxidation products **VII** and **VIII** were also detected under irradiation but with maximum amounts below 3.5% AR. Although their formation was of minor importance in the dark (<1% AR), an increased amount of **VII** was

observed during TLC development, suggesting oxidation of **I** by atmospheric ozone.[10,18,19] Cleavage of the ester linkage proceeded to a similar extent under irradiated and dark conditions. Under irradiation, **VI** gradually increased to 8.7% AR at 9 days, probably formed via stepwise oxidation at the benzyl carbon of **IV** through **V**, but the corresponding acids **II** and **III** were detected only in trace amounts (<1.2% AR) throughout the study. Because mineralization to CO_2 from the CP-label samples was more significant than that from those with the PP-label, **II** was most likely to be rapidly degraded under the test conditions. Selected acidic/exhaustive extracts from the irradiated samples contained mainly **III** (2.8% AR) and **IV** (4.7% AR) as well as multiple degradates at low levels. Chiral HPLC analysis of the isolated parent fraction gave the single dominant peak of **I** with trace amounts of the other isomers (<1.4% AR) at any point, indicating that photoinduced isomerization was of minor importance throughout the study.

Detection of Singlet Oxygen ($^1O_2$). After 7 h of irradiation, three bands were evident at HPLC retention times of 9.8, 10.8, and 12.4 min, as shown in Figure 3a. They were similarly observed for photolysis of the aqueous solution containing RB after 1 h of irradiation (Figure 3b), but not detected in the absence of RB or in the dark control (data not shown). On the basis of the same molecular weight of 112 amu (m/z 113 $[M + H]^+$ and 111 $[M - H]^-$) and their reported HPLC retention times,[5] the former two bands could be assigned as *cis*- (CDE) and *trans*-diacetylethylene (TDE) eluting in sequence. The third band at 12.4 min may be assigned as the ozonide intermediate, which is the precursor of CDE and TDE (Figure 4) on the basis of its molecular weight of 128 amu, as evidenced by the LC-APCI-MS signal at m/z 129 $[M + H]^+$. It has been reported that sterically hindered amines such as TMPD are selectively oxidized by $^1O_2$ to form their corresponding nitroxide radicals. As shown in Figure 5b,c, the ESR spectra of TMPD aqueous solutions containing OMs and HA fractions showed triplet signals after 15 min of irradiation. These equal-intensity signals are correctly assigned as the nitroxide radical of TMPD, 2,2,6,6-tetramethyl-4-piperidone-*N*-oxyl radical, with A_N = 1.58 mT and g value = 2.0057. As for the irradiated solution without added soil-extracted fractions, ESR signals were not detected (Figure 5a). Furthermore, the addition of an efficient $^1O_2$ scavenger sodium azide (NaN_3) markedly decreased the formation of the nitroxide radical (Figure 5d). These results clearly indicate the photoinduced generation of $^1O_2$ with the aid of soil OMs, especially HA.

DISCUSSION

The net photodegradation half-lives of **I** on the soil thin layer were calculated to be 7.5−8.2 days from the first-order degradation half-lives of 5.7−5.9 days (light) and 21−24 days (dark). The photodegradation rates of **I** in the real environment were estimated according to the OECD draft soil photolysis guideline[28] by using the midday sunlight intensity of summer months at 30−50° N latitude in the range of 300−400 nm (67 W/m^2). Using the converted photolytic rate constants taking into account the dark reaction, the photodegradation half-life of **I** was estimated to be 8.5 days at 30−50° N latitude (summer), indicating the rapid dissipation of **I** on an environmental soil surface under natural sunlight.

On the basis of the identification of photoproducts by cochromatography with authentic reference standards and LC-MS analyses, the photodegradation pathways of **I** on soil surfaces are shown in Figure 6. On exposure to light, **I** underwent either photoinduced oxidation or ester cleavage as reported in the analogous pyrethroids, tetramethrin and resmethrin.[7,8] Photoinduced isomerization via homolytic cleavage of the C_1-C_3 bond in the cyclopropane ring was of minor importance, indicating that the oxidation reaction predominated rather than the formation of 1,3-diradical intermediates generated from the excited triplet state of the ester carbonyl.[29] Even though ether cleavage and hydroxylation at the 4′-position of the phenoxyphenyl ring were not observed in contrast to results from a previous aerobic soil metabolism,[14] the similar extent of ester cleavage observed irrespective of irradiation supports the involvement of microbial degradation on the soil thin layer. The corresponding acids (**II** and **III**) formed via ester cleavage were likely to be more unstable than **VI**, and their rapid degradation through the opening of the cyclopropane ring followed by successive oxidation would result in greater evolution of CO_2 from the CP-label by irradiation or microbial degradation, as also reported for the dichlorovinyl chrysanthemic acid analogues.[30−32] These findings imply that the contribution of direct photolysis of **I** through direct absorption of the light[33] is unlikely due to the attenuation and scattering of the light by soil particles or organic matter.

Therefore, it would appear that the main degradation route of **I** on soil surfaces is photoinduced oxidation mainly via indirect photolysis involving reactive oxygen species. A significant increase of the allylic alcohol (**IX**) and ketone (**X**) derivatives under irradiation indicates that the photogenerated $^1O_2$ is the most likely reactant because these distinctive products would form from the hydroperoxide intermediate via the ene reaction.[7] The involvement of $^1O_2$ is also supported by the slight increase observed in the corresponding aldehyde (**VII**) and carboxylic acid (**VIII**) formed through an unstable dioxetane intermediate via cycloaddition at the 2-methylprop-1-enyl moiety. As an alternative route, atmospheric ozone may partially contribute to the formation of **VII** and **VIII**, which has been reported as one of the major photolytic pathways in oxygenated benzene solution, on thin films and on plant leaf surfaces through the ozonide intermediate.[7,14,19] Although their formation was of minor importance in the present study, the slight increase of **VII** and **VIII** under the irradiation conditions may also be attributed to the enhancement of ozonolysis by light, as demonstrated in our recent investigation of methofluthrin.[11]

The preferential formation of **IX** and **X** on soil surfaces strongly indicates that photogenerated $^1O_2$ plays an important role in the degradation of **I**, as previously reported in the photodegradation behavior of thioether-containing pesticides.[34] Although the steady-state concentration of $^1O_2$ has been reported to be $10^{-14}-10^{-12}$ M in natural waters with rapid quenching in 3−5 μs to the ground state by water,[4,35] it is conceivable that $^1O_2$ might be of greater importance on soil surfaces and in hydrophobic environments such as surface microlayers or petroleum films, in which its lifetime would be longer.[36] Furthermore, HSs, which are the most widely distributed OMs in terrestrial soil, can serve as photosensitizers to yield $^1O_2$ via a triplet energy transfer process to molecular oxygen.[37−39] First, the detection of $^1O_2$ was investigated by using the effective trapping agent DMF, giving the corresponding *endo*-peroxide as an ozonide.[21] The appearance of the resultant diketoenes CDE and TDE as well as their precursor ozonide implies that $^1O_2$ was generated under the irradiation conditions (Figures 3 and 4). Lesser amounts of ozonide were observed on soil surfaces as compared with solutions of the

photosensitizer dye RB, possibly due to its rapid reduction as previously reported.[5] Meanwhile, the formation of the potent oxidant hydroxyl radical ($^{\bullet}$OH), the generation of which is reported via photocatalytic or photosensitized reaction from soil clay minerals or HSs, can be inferred because furan derivatives such as DMF are known to react with $^{\bullet}$OH to mainly form the same diketoene products but not the *endo*-peroxide.[40] Although the contribution of $^{\bullet}$OH is unclear due to the less selective character of furan derivatives, subsequent experiments using $^1O_2$-specific spin label TMPD combined with ESR spectroscopy provided robust evidence for the presence of $^1O_2$ upon irradiation. As shown in Figure 5, the apparent ESR signals assigned as the resultant nitroxide radical were detected in the soil-extracted OMs and HA fraction under irradiation. These findings indicated that OMs extracted from soil act as energy-transfer agents toward molecular oxygen, in particular, the HA fraction is considered to be the principal photosensitizer leading to $^1O_2$ formation.

In conclusion, the degradation of the predominant 1*R-trans*-isomer of phenothrin (**I**) was accelerated by light irradiation, and the photoinduced oxidation at the 2-methylprop-1-enyl side chain of the acid moiety preferentially proceeded as the major degradation pathway on soil surface. The photosensitized generation of $^1O_2$ in the presence of soil OMs was clearly demonstrated by using chemical-trapping agents combined with ESR spectroscopy, and this electrophilic oxygen species plays an important role in the oxidation process. In addition to the rapid dissipation of **I**, the declines of oxidative degradates with concomitant mineralization (CO_2 formation) at the latter samplings indicate that they are unlikely to persist on soil surfaces when phenothrin is released into the environment.

REFERENCES

(1) Miller, G. C.; Zepp, R. G. Extrapolating photolysis rates from the laboratory to the environment. *Residue Rev.* **1983**, *85*, 89–110.

(2) Katagi, T. Photodegradation of pesticides on plant and soil surfaces. *Rev. Environ. Contam. Toxicol.* **2004**, *182*, 1–195.

(3) Zepp, R. G.; Wolfe, N. L.; Baughman, G. L.; Hollis, R. C. Singlet oxygen in natural waters. *Nature* **1977**, *267*, 421–423.

(4) Haag, W. R.; Hoigné, J. Singlet oxygen in surface waters. 3. Photochemical formation and steady-state concentrations in various types of waters. *Environ. Sci. Technol.* **1986**, *20*, 341–348.

(5) Gohre, K.; Miller, G. C. Singlet oxygen generation on soil surfaces. *J. Agric. Food Chem.* **1983**, *31*, 1104–1108.

(6) Gohre, K.; Scholl, R.; Miller, G. C. Singlet oxygen reactions on irradiated soil surfaces. *Environ. Sci. Technol.* **1986**, *20*, 934–938.

(7) Ruzo, L. O.; Smith, I. H.; Casida, J. E. Pyrethroid photochemistry: photooxidation reactions of the chrysanthemates phenothrin and tetramethrin. *J. Agric. Food Chem.* **1982**, *30*, 110–115.

(8) Ueda, K.; Gaughan, L. C.; Casida, J. E. Photodecomposition of resmethrin and related pyrethroids. *J. Agric. Food Chem.* **1974**, *22*, 212–220.

(9) Clements, P.; Wells, C. H. J. Soil sensitized generation of singlet oxygen in the photodegradation of bioresmethrin. *Pestic. Sci.* **1992**, *34*, 163–166.

(10) Ruzo, L. O.; Kimmel, E. C.; Casida, J. E. Ozonides and epoxides from ozonization of pyrethroids. *J. Agric. Food Chem.* **1986**, *34*, 937–940.

(11) Nishimura, H.; Suzuki, Y.; Nishiyama, M.; Fujisawa, T.; Katagi, T. Photodegradation of insecticide methofluthrin on soil, clay minerals and glass surfaces. *J. Pestic. Sci.* **2011**, *36*, 376–384.

(12) Fujimoto, K.; Itaya, N.; Okuno, Y.; Kadota, T.; Yamaguchi, T. A new insecticidal pyrethroid ester. *Agric. Biol. Chem.* **1973**, *37*, 2681–2682.

(13) Okuno, Y.; Yamaguchi, T.; Fujita, Y. Insecticidal activity of a new synthetic pyrethroidal compound, 3-phenoxy benzyl-(+) *cis*, *trans* chrysanthemate (*d*-phenothrin). *Bochu-Kagaku* **1976**, *41*, 42–55.

(14) Nambu, K.; Ohkawa, H.; Miyamoto, J. Metabolic fate of phenothrin in plants and soils. *J. Pestic. Sci.* **1980**, *5*, 177–197.

(15) Nambu, K.; Takimoto, Y.; Miyamoto, J. Degradation of phenothrin in stored wheat grains. *J. Pestic. Sci.* **1981**, *6*, 183–191.

(16) Kaneko, H.; Ohkawa, H.; Miyamoto, J. Absorption and metabolism of dermally applied phenothrin in rats. *J. Pestic. Sci.* **1981**, *6*, 169–182.

(17) Miyamoto, M.; Saito, S.; Takimoto, Y.; Matsuo, M. Effect of metabolism on bioconcentration of geometric isomers of *d*-phenothrin in fish. *Chemosphere* **1992**, *24*, 2001–2007.

(18) Class, T. J. Determination of pyrethroids and their degradation products in indoor air and on surfaces by HRGC-ECD and HRGC-MS (NCI). *J. High Resolut. Chromatogr.* **1991**, *14*, 446–450.

(19) Class, T. J. Gas chromatographic and mass spectrometric studies on pyrethroid photo- and biotransformation. *Fresenius' J. Anal. Chem.* **1992**, *342*, 805–808.

(20) Foote, C. S. Photosensitized oxygenations and the role of singlet oxygen. *Acc. Chem. Res.* **1968**, *1*, 104–110.

(21) Gleason, W. S.; Broadbent, A. D.; Whittle, E.; Pitts, J. N., Jr. Singlet oxygen in the environmental sciences. IV. Kinetics of the reactions of oxygen ($^1\Delta_g$) with tetramethylethylene and 2,5-dimethylfuran in the gas phase. *J. Am. Chem. Soc.* **1970**, *92*, 2068–2075.

(22) Lion, Y.; Delmelle, M.; Van de Vorst, A. New method of detecting singlet oxygen production. *Nature* **1976**, *263*, 442–443.

(23) Moan, J.; Wold, E. Detection of singlet oxygen production by ESR. *Nature* **1979**, *279*, 450–451.

(24) Nagase, T.; Suzukamo, G.; Fukao, M.; Sakito, Y. Interconversion of optical isomers of chrysanthemic acid and related reactions. *Sumitomo Kagaku* **1983**, *I*, 25–31.

(25) Matsui, M.; Uchiyama, M.; Yoshioka, H. Studies on chrysanthemic acid. Part XI. Oxidation products from chrysanthemic acid, 2,2-dimethyl-3-(1′-oxo-2′-hydroxy-2′-methyl)propyl-1,3-*trans*-cyclopropane-1-carboxylic acid. *Agric. Biol. Chem.* **1963**, *27*, 554–557.

(26) Piancatelli, G.; Scettri, A.; D'auria, M. Pyridinium chlorochromate: a versatile oxidant in organic synthesis. *Synthesis* **1981**, *1*, 245–258.

(27) Swift, R. S. Organic matter characterization (Chapter 35). In *Methods of Soil Analysis. Part 3. Chemical Methods*; Sparks, D. L., Page, A. L., Helmke, P. A., Loeppert, R. H., Soltanpour, P. N., Tabatabai, M. A., Johnston, C. T., Sumner, M. E., Eds.; Soil Science Society of America: Madison, WI, 1996; pp 1011−1069 [International Humic Substance Society (http://www.ihss.gatech.edu/)].

(28) Phototransformation of chemicals on soil surfaces, draft document. *OECD Guidelines for the Testing of Chemicals*; Jan 2002.

(29) Ruzo, L. O.; Casida, J. E. Pyrethroid photochemistry: mechanistic aspects in reactions of the (dihalogenovinyl)cyclopropanecarboxylate substituent. *J. Chem. Soc., Perkin Trans. 1* **1980**, *3*, 728–732.

(30) Holmstead, R. L.; Casida, J. E.; Ruzo, L. O.; Fullmer, D. G. Pyrethroid photodecomposition: permethrin. *J. Agric. Food Chem.* **1978**, *26*, 590–595.

(31) Roberts, T. R.; Standen, M. E. Further studies of the degradation of the pyrethroid insecticide cypermethrin in soils. *Pestic. Sci.* **1981**, *12*, 285–296.

(32) Sakata, S.; Mikami, N.; Yamada, H. Degradation of pyrethroid optical isomers in soils. *J. Pestic. Sci.* **1992**, *17*, 169–180.

(33) Fernández-Álvarez, M.; Lores, M.; Llompart, M.; García-Jares, C.; Cela, R. The photochemical behaviour of five household pyrethroid insecticides and a synergist as studied by photo-solid-phase microextraction. *Anal. Bioanal. Chem.* **2007**, *388*, 1235–1247.

(34) Gohre, K.; Miller, G. C. Photooxidation of thioether pesticides on soil surfaces. *J. Agric. Food Chem.* **1986**, *34*, 709–713.

(35) Gorman, A. A.; Rodgers, M. A. J. Singlet oxygen (Chapter 10). In *Handbook of Organic Photochemistry*; Scaiano, J. C., Ed.; CRC Press: Boca Raton, FL, 1989; Vol. II, pp 229−247.

(36) Larson, R. A.; Weber, E. J. Environmental oxidations (Chapter 4). In *Reaction Mechanisms in Environmental Organic Chemistry*; Lewis Publishers: Boca Raton, FL, 1994; pp 217−273.

(37) Slawinski, J.; Puzyna, W.; Slawinski, D. Chemiluminescence during photooxidation of melanins and soil humic acids arising from a singlet oxygen mechanism. *Photochem. Photobiol.* **1978**, *267*, 459–463.

(38) Aguer, J. P.; Richard, C.; Andreux, F. Comparison of the photoinductive properties of commercial, synthetic and soil-extracted humic substances. *J. Photochem. Photobiol., A* **1997**, *103*, 163–168.

(39) Paul, A.; Hackbarth, S.; Vogt, R. D.; Röder, B.; Burnison, B. K.; Steinberg, C. E. W. Photogeneration of singlet oxygen by humic substances: comparison of humic substances of aquatic and terrestrial origin. *Photochem. Photobiol. Sci.* **2004**, *3*, 273–280.

(40) Noguchi, T.; Takayama, K.; Nakano, M. Conversion of 2, 5-dimethylfuran to 2-hydroxy-5-hydroperoxy-2,5-dimethyldihydrofuran, a true $^1O_2$-derived reaction in aqueous $^1O_2$ generating systems. *Biochem. Biophys. Res. Commun.* **1977**, *78*, 418–423.